CORRIGENDUM

Development 140, 481 (2013) doi:10.1242/dev.092395

Neural tube patterning by Ephrin, FGF and Notch signaling relays

Alberto Stolfi, Eileen Wagner, J. Matthew Taliaferro, Seemay Chou and Michael Levine

There was an error published in *Development* **138**, 5429-5439.

On p. 5431, PIPES-sucrose-FA buffer was incorrectly described. The correct composition of this buffer is: 400 mM sucrose, 50 mM EGTA, 100 mM PIPES pH 7, 4% formaldehyde.

The authors apologise to readers for this mistake.

Development 138, 5429-5439 (2011) doi:10.1242/dev.072108

Neural tube patterning by Ephrin, FGF and Notch signaling relays

Alberto Stolfi*, Eileen Wagner, J. Matthew Taliaferro, Seemay Chou and Michael Levine

SUMMARY

The motor ganglion (MG) controls the rhythmic swimming behavior of the *Ciona intestinalis* tadpole. Despite its cellular simplicity (five pairs of neurons), the MG exhibits conservation of transcription factor expression with the spinal cord of vertebrates. Evidence is presented that the developing MG is patterned by sequential Ephrin/FGF/MAPK and Delta/Notch signaling events. FGF/MAPK attenuation by a localized EphrinAb signal specifies posterior neuronal subtypes, which in turn relay a Delta2/Notch signal that specifies anterior fates. This short-range relay is distinct from the patterning of the vertebrate spinal cord, which is a result of opposing BMP and Shh morphogen gradients. Nonetheless, both mechanisms lead to localized expression of related homeodomain codes for the specification of distinct neuronal subtypes. This MG regulatory network provides a foundation for elucidating the genetic and cellular basis of a model chordate central pattern generator.

KEY WORDS: *Ciona*, Ephrin, FGF, Motoneurons, Neural tube, Notch

INTRODUCTION

Central pattern generators (CPGs) are discrete neuronal networks that drive rhythmic motor behaviors (Marder and Bucher, 2001; Wilson and Maden, 2005). Spinal cord CPGs control the swimming behavior of lampreys and fish and the repetitive movements of amniote limbs. They are composed of motoneurons and interneurons that are assembled into 'motor pools' innervating specific muscles. Understanding how neuronal subtypes interconnect to control locomotion has become an intensive area of research (Goulding, 2009).

Sea squirts, or ascidians, belong to the Urochordates, the sister group to the vertebrates (Delsuc et al., 2006). The tadpole larvae of *Ciona intestinalis* possess a typical chordate body plan with a central nervous system (CNS) composed of only ~100 neurons (Meinertzhagen et al., 2004; Nicol and Meinertzhagen, 1991). Most of these neurons are dedicated to the swimming behavior of the tadpole, a crucial process as this is the only motile phase of the ascidian life cycle (Kajiwara and Yoshida, 1985; Mackie and Bone, 1976). The numerous advantages of *Ciona* as an experimental organism include a compact genome, invariant cell lineages, rapid development and simple transgenesis methods (Lemaire, 2011; Satoh, 2003). The cellular simplicity of the *Ciona* CNS makes it an ideal model for understanding the development and function of chordate-specific neuronal networks (Meinertzhagen et al., 2004; Meinertzhagen and Okamura, 2001).

The motor ganglion (MG) controls the swimming behavior of the tadpole. It is situated at the base of the tail in the trunk (hence the alternative term 'trunk ganglion') and was originally called the 'visceral ganglion' despite the absence of contacts with viscera (Grave, 1921). The MG contains five bilaterally symmetrical pairs of cholinergic neurons that project their axons along the muscle bands in the tail (Fig. 1A) (Horie et al., 2010; Takamura et al., 2002; Takamura et al., 2010). Together with commissural glycinergic inhibitory interneurons in the nerve cord, they drive the alternating left-right contractions of the tail that propel the tadpole forward. This behavior is retained by dissected preparations containing only the MG, nerve cord and tail (Brown et al., 2005; Nishino et al., 2010).

Each of the five pairs of MG neurons are morphologically distinct and express a particular homeodomain 'code' (Ikuta and Saiga, 2007; Imai and Meinertzhagen, 2007; Imai et al., 2009; Stolfi and Levine, 2011). We will hereafter refer to these pairs of neurons as single cells on one side of the embryo. The neurons of the MG, from anterior to posterior, are A12.239, A13.474, A11.118, A11.117 and A10.57 (Fig. 1F). A conserved motoneuron 'code' of Lhx3-Islet-Mnx suggests the occurrence of two primary motoneurons (A11.118 and A10.57) (Lee et al., 2008; Thaler et al., 2002; Thor et al., 1999). A11.118 forms prominent neuromuscular endplates (Fig. 1B). Putative interneurons A13.474 and A11.117 express Vsx (also known as Chx10), which specifies V2 spinal interneurons in vertebrates. A11.117 also expresses *Pitx* (Fig. 1C) (Stolfi and Levine, 2011), suggesting similarity to *Pitx2*+ cholinergic v0 interneurons in the vertebrate spinal cord (Zagoraiou et al., 2009). Lastly, the decussating A12.239 neuron expresses *Dmbx* (Fig. 1D) (Takahashi and Holland, 2004), *Lhx1/5* and *PouIV* and might be related to an uncharacterized subset of v0 interneurons in the vertebrate spinal cord (Ohtoshi and Behringer, 2004).

Vertebrate neuronal subtypes are established along the dorsal-ventral (DV) axis by opposing bone morphogenetic protein (BMP) and Shh signaling gradients (Briscoe and Novitch, 2008; Briscoe et al., 1999; Ericson et al., 1996; Ericson et al., 1997; Lee et al., 2000). This mechanism does not pattern the *Ciona* MG, despite conserved expression of BMP2/4 and Shh in the *Ciona* neural tube (Hudson et al., 2011). We recently presented evidence that fibroblast growth factor (FGF) and Notch signaling specify different MG neuronal subtypes (Stolfi and Levine, 2011). Here, we present evidence that Ephrin/Eph-mediated inhibition of FGF signaling in progenitors of the posterior MG leads to the localized

Department of Molecular and Cell Biology, Division of Genetics, Genomics and Development, Center for Integrative Genomics, University of California, Berkeley, CA 94720, USA.

*Author for correspondence (albertostolfi@gmail.com)

Accepted 19 October 2011

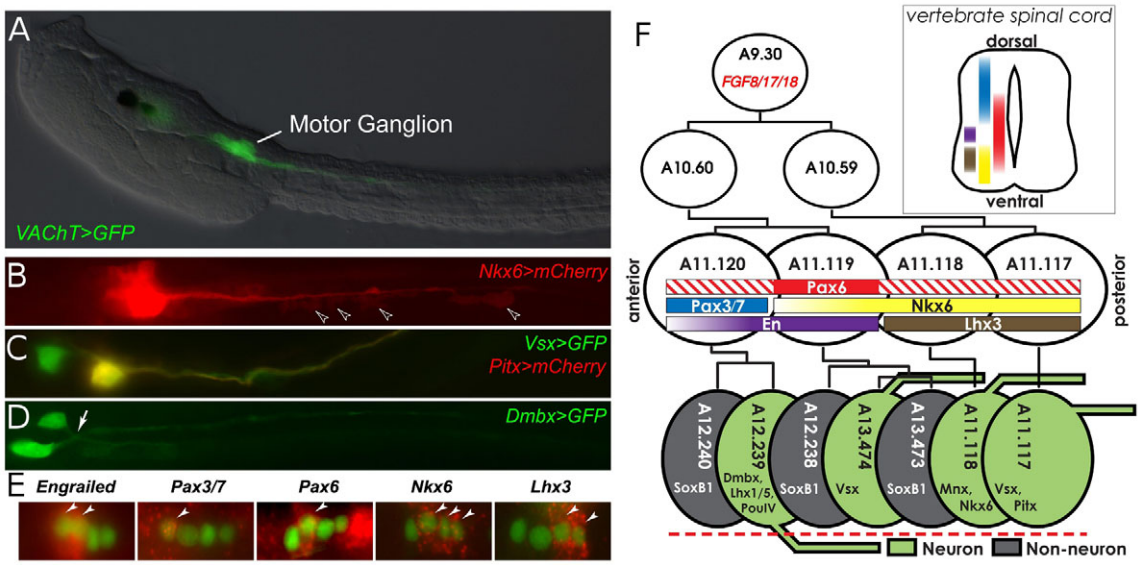

Fig. 1. Development and morphology of motor ganglion neuronal subtypes in *Ciona*. (**A**) Visualization of the MG by *VACHT>GFP* cholinergic reporter. (**B**) Visualization of A11.118-specific frondose endplates (arrowheads) by *Nkx6>mCherry*. Broad staining in the MG is due to early Nkx6 throughout the lineage. Nkx6 expression is later restricted to A11.118 motoneuron. (**C**) Visualization of A13.474 and A11.117 interneurons by co-electroporation of *Vsx>GFP* (green) and *Pitx>mCherry* (red). *Vsx* is expressed in both neurons, whereas *Pitx* is expressed only in A11.117 (yellow). (**D**) Visualization of A12.239 neuron pair by *Dmbx>GFP*. Note commissure resulting from A12.239 axons crossing the midline (arrow). (**E**) In situ hybridization of factors shown in F. Arrowheads denote gene expression. Nuclei of the A9.30 lineage are visualized by immunofluorescence detection of nuclear β-galactosidase reporter (green) driven by the *FGF8/17/18* driver (*FGF8/17/18>lacZ*). (**F**) Diagram of the A9.30 lineage. *FGF8/17/18* is expressed in A9.30 and is a marker for the lineage through visualization of *FGF8/17/18* reporter. Homeobox transcription factor gene expression at the four-cell stage of the lineage is denoted by colored bars. 'Fading out' of colored bars represents weak/transient expression. Hashed fill indicates previous expression in the lineage. Gene expression in differentiated neurons born from the lineage is indicated at the bottom. Inset: diagram comparing A9.30 lineage gene expression to expression of orthologs of *Pax3/7* (*Pax3* and *Pax7*), *Pax6*, *Nkx6* (*Nkx6.1* and *Nkx6.2*), *En* and *Lhx3* along the DV axis of the vertebrate spinal cord. Based on Briscoe et al. (Briscoe et al., 2000). Anterior is to the left in all images.

activation of Notch signaling in the anterior MG. This FGF-Notch signaling relay leads to sequential homeodomain codes along the anterior-posterior (AP) axis that are similar to the DV patterning domains seen in the vertebrate spinal cord. Thus, divergent signaling strategies are used to specify related neuronal subtypes in the *Ciona* MG and vertebrate spinal cord.

MATERIALS AND METHODS

Molecular cloning

Templates for in vitro transcription of RNA probes are from the *Ciona intestinalis* Gene Collection Release 1 (http://ghost.zool.kyoto-u.ac.jp/indexr1.html) (Satou et al., 2005; Satou et al., 2002), with plate/well identifiers cross-referenced to annotation on the ANISEED database (Tassy et al., 2010): *HesB* (04g10), *Ngn* (29n04), *Mnx* (42o14), *Lhx1/5* (44f09), *Lhx3* (25m02), *En* (28a10), *PouIV* (32g05), *Pax3/7* (42e20), *Delta2* (16e18), *SoxB1* (01k09). Template for *EphrinAb* probe was made by cloning the full-length coding sequence (see below) into the same backbone as the other gene collection clones. Templates for *Pax6*, *Nkx6*, *Dmbx* and *Vsx* riboprobes were constructed previously (Stolfi and Levine, 2011).

En reporter was constructed using a fragment –2085 to +24 bp from the translation start of *En*. *FGF8/17/18*. *Dmbx*, *Vsx* and *Msx* reporters were described previously (Russo et al., 2004; Stolfi and Levine, 2011). *Dmbx* minimal enhancer from *C. intestinalis* was PCR-amplified with the following primers: Dmbx min F: TTTGTGACGTCACGCCTTAAC; Dmbx min R: AGTACTATGACGTTACAATCC. *Dmbx* minimal enhancer from *C. savignyi* was PCR-amplified with the following primers: Dmbx-Cs min F: CACTTTCCGAATCAACGTCC; Dmbx-Cs min R: TTGTCTGTCTCTGCGTACGTC.

Eph3ΔC was constructed by removing the intracellular C-terminus of Eph3, leaving amino acid (aa) residues 1-579 (Picco et al., 2007). *Eph1ΔC* (aa 1-616), *Eph2ΔC* (aa 1-612), *Eph4ΔC* (aa 1-611) and *Eph-likeΔC* (aa 1-683) were similarly designed and constructed. Nomenclature is according to the list of RTK genes on the Ghost database (Satou et al., 2005). Constitutively active *Eph3* (*caEph3*) was made by fusing the C-terminal transmembrane and intracellular domains (aa 512-1027) of Eph3 to the self-dimerizing N-terminus (aa 1-391) of *Drosophila* Torso receptor tyrosine kinase (Sprenger and Nusslein-Volhard, 1992). *EphrinAb*, *Pax3/7* and *Pax6* were cloned from a tailbud embryo cDNA library. Coding sequences of *Ngn*, *SoxB1* and all other Ephrins [*EphrinAa* (41n20), *EphrinAc* (07i06), *EphrinAd* (01j20)] were taken from collection clones. Ngn::WRPW was constructed by fusing the bHLH domain (aa 84-173) to a Groucho-recruitment WRPW motif (aa 326-337) from *Drosophila* Hairy (Wainwright and Ish-Horowicz, 1992). Pax3/7::WRPW was made by fusing the N-terminal paired box and homeodomain (aa 3-253) to WRPW. Pax3/7::VP16 was made by fusing aa 3-253 to the transactivation domain of the Herpes virus VP16 activator (aa 413-490) (Rusch and Levine, 1997). Dmbx::WRPW was made by fusing the first 116 amino acid residues from Dmbx to the WRPW motif. *dnFGFR*, *caFGFR*, *Su(H)-DBM* and *Delta2* constructs have been described (Davidson et al., 2006; Hudson and Yasuo, 2006; Pasini et al., 2006; Shi and Levine, 2008).

Embryo electroporation

Animals were obtained from Pillar Point Marina (Half Moon Bay, CA, USA) or ordered from M-Rep (San Diego, CA, USA). Embryos were manipulated as previously described (Christiaen et al., 2009) and grown at 20°C, unless otherwise stated.

Control embryos for fluorescent protein-based assays were electroporated with *lacZ* plasmids to control for transfection load. Control embryos for in situ hybridizations were electroporated with *GFP/mCherry*

plasmids. For experiments in which increased dose of perturbation was desired, plasmid concentration was simply increased, with transfection load equalized by co-electroporation with *lacZ* plasmids.

Images were photographed using a Zeiss AxioImager A.2 upright compound microscope, a Leica SP2 upright confocal microscope or a Zeiss700 inverted confocal microscope.

Inhibitor treatments

U0126 (Promega) and DAPT (Enzo Life Sciences) were resuspended in DMSO and diluted in seawater to 10 μM and 100 μM, respectively. Both were added to seawater immediately prior to the start of treatment, to minimize precipitation. Control embryos were treated with DMSO alone.

In situ hybridization and immunohistochemistry

Fluorescence in situ hybridization was performed as described (Beh et al., 2007). Two-color in situ hybridizations were performed by labeling one probe with digoxigenin-UTP and the other with fluorescein-UTP. Sequential TSA-plus (Perkin-Elmer) tyramide-based detection using peroxidase domain (POD)-conjugated anti-digoxigenin and anti-fluorescein Fab fragments (Roche) was performed with a 10 minute 0.01 N HCl inactivation step between the first probe detection and incubation with the second POD conjugate. β-Galactosidase detection was carried out using mouse anti-β-galactosidase primary (1:1000, Promega #Z378) and Alexa Fluor-conjugated secondary antibodies (1:1000, Invitrogen).

For dpMAPK detection, embryos were fixed in a PIPES-sucrose-FA buffer (2 M sucrose, 0.5 EGTA, 0.5 M PIPES, 10% formaldehyde) for 30-60 minutes at room temperature. Fixed embryos were quenched with 0.3% H_2O_2 in 0.3% horse serum/PBS/Tween for 30 minutes and incubated with monoclonal mouse anti-dpERK primary antibody (1:500, Sigma #M9692). Embryos were then incubated with biotinylated horse anti-mouse IgG (Vector Laboratories #BA-2000) and avidin-biotin-peroxidase complexes using Vectastain Elite ABC Reagent R.T.U. kit (Vector Laboratories), according to the manufacturer's recommendations. TSA-plus amplification was carried out as recommended. Co-detection of β-galactosidase was performed using rabbit anti-β-galactosidase (1:1000, Invitrogen #A-11132), coupled to Alexa Fluor-conjugated secondary (1:1000).

When counterstaining certain embryos, fluorophore-conjugated phalloidin or phallicidin (1:200-1:500, Invitrogen) was used to reveal cell shape or Hoechst (1:1000-1:4000, Invitrogen) to stain nuclei.

Pax3/7 expression and purification

A Pax3/7 fragment lacking the disordered C-terminal region (Pax3/7ΔC, residues 3-259) was cloned into pRSETB (Invitrogen) for expression in *Escherichia coli*. pRSETB-Pax3/7ΔC was transformed into BL21-CodonPlus cells (Agilent) and grown in 2 liters of TB. Expression was induced at optical density (OD) 0.6 with 100 μM IPTG and grown for an additional 16 hours at 16°C. Cells were harvested by centrifugation and resuspended in Ni-A Buffer (20 mM HEPES pH 7.5, 300 mM NaCl, 10% glycerol, 0.5 mM TCEP, 25 mM imidazole, 50 mM AEBSF). Following sonication at 4°C, lysate was cleared by centrifugation at 15,000 ***g*** for 45 minutes, and $(His)_6$-Pax3/7ΔC was eluted with Ni-B Buffer (20 mM HEPES pH 7.5, 300 mM NaCl, 10% glycerol, 0.5 mM TCEP, 350 mM imidazole) from 5 ml His-Trap Nickel Column (GE) using AKTA-Explorer FPLC (GE). Fractions containing $(His)_6$-Pax3/7ΔC were identified by SDS-PAGE, pooled and purified by size exclusion chromatography using analytical S200 Column in Buffer-200 (200 mM NaCl, 20 mM HEPES pH 7.5, 5% glycerol and 0.5 mM TCEP). $(His)_6$-Pax3/7ΔC eluted at a molecular weight of 31 kDa. Fractions containing soluble, monomeric $(His)_6$-Pax3/7ΔC were pooled and concentrated to 2 mg/ml.

Electrophoretic mobility shift assay (EMSA)

Oligonucleotides (26-mer) containing the wild-type (GCGCGAAAT) or mutant (GGCCGAAAT) Pax3/7 binding site (Elim Biopharmaceuticals) and their respective complements were annealed by mixing 10 pmol of each oligo in a buffer containing 10 mM Tris pH 7.5 and 100 mM NaCl. The reaction was heated to 95°C for 5 minutes and allowed to cool slowly to room temperature over 1 hour. The oligonucleotides were labeled with γ-^{32}P-ATP and Optikinase (USB) following the manufacturer's instructions. The reactions were spun twice through P-6 columns (Bio-Rad) to remove free nucleotides.

EMSAs were performed using standard procedures. For non-competition assays, purified Pax3/7ΔC was serially diluted to create stocks of 10 μM to 304 pM. Ten microliters of each stock was mixed with 10 μl of buffer containing labeled oligonucleotide for final protein concentrations ranging from 5 μM to 152 pM. The binding reaction conditions were 20 mM HEPES pH 7.6, 125 mM KCl, 0.2 mM EDTA, 0.5 mM DTT, 4 mM $MgCl_2$, 0.1 nM oligonucleotide (~2500 cpm). Reactions were incubated at room temperature for 45 minutes and run on a 5% native polyacrylamide gel (60:1 acrylamide:bis acrylamide) in 0.5× TBE for 2 hours at 180 V, 4°C. Gels were dried and visualized using a Typhoon phosphorimager (GE).

For the assays containing non-specific competitor DNA, reactions were set up and performed as above with the following exceptions: reactions contained motif-containing oligonucleotide at 0.1 nM and 2.5 ng/μl poly[dI-dC] (1500-fold excess) and the final protein concentrations in each reaction ranged from 62.5 μM to 2.5 nM in twofold steps.

RESULTS

Similar homeodomain codes in the *Ciona* MG and vertebrate spinal cord

The invariant lineages that produce the five pairs of MG neurons have been described in detail (Cole and Meinertzhagen, 2004). The A9.30 lineage produces four of the five neurons, whereas the A10.57 motoneuron arises from the more posterior A9.29 lineage (Fig. 1F). These neurons exhibit partially overlapping domains of expression of *Engrailed* (*En*), *Pax3/7*, *Pax6*, *Nkx6* and *Lhx3* along the AP axis, similar to the DV patterning of the vertebrate spinal cord (Fig. 1E) (Briscoe et al., 2000; Imai et al., 2009).

Localized expression of BMP and Shh establishes these DV homeodomain codes in the vertebrate spinal cord. Although BMP and Shh exhibit similar DV expression profiles in the *Ciona* neural tube, they are not required for MG neuronal specification (Hudson et al., 2011). Instead, FGF and Notch signaling appear to control this process. We recently showed that targeted expression of a dominant negative FGF receptor (dnFGFR) causes the A9.30 lineage to produce only A11.117 interneurons (the posterior-most identity within the A9.30 lineage). Moreover, targeted expression of a dominant negative form of Su(H), the transcriptional effector of Notch signaling, resulted in the duplication of A12.239 decussating neurons (Stolfi and Levine, 2011). In the present study, we sought to determine how FGF and Notch signaling work in concert to pattern the *Ciona* MG.

Early inhibition of MAPK results in an anterior-to-posterior transformation

Progressively older embryos were treated with the irreversible MEK (MAPKK) inhibitor U0126 (Fig. 2A,B). Expression of *En*, *Mnx* and *Vsx* was monitored using two-color fluorescence in situ hybridization, to assess the fate of A9.30 daughter cells (A10.60 and A10.59) and granddaughter cells (A11.120, A11.119, A11.118, A11.117). *En* is expressed in A11.120 and A11.119, whereas *Mnx* and *Vsx* are expressed in A11.118 and A11.117, respectively. Early application of U0126 [6 hours post-fertilization (hpf)] causes Vsx to be expressed in all four granddaughter cells rather than being restricted to the posterior-most A11.117 neuron. We interpret this result as the transformation of A10.60 into A10.59, followed by the conversion of A11.118 to the A11.117 fate (Fig. 2C).

By contrast, treatment of older embryos with U0126, at 7 and 8 hpf, does not abolish *En* expression. Instead, *Vsx* is ectopically expressed only in A11.118, at the expense of *Mnx* (transformation

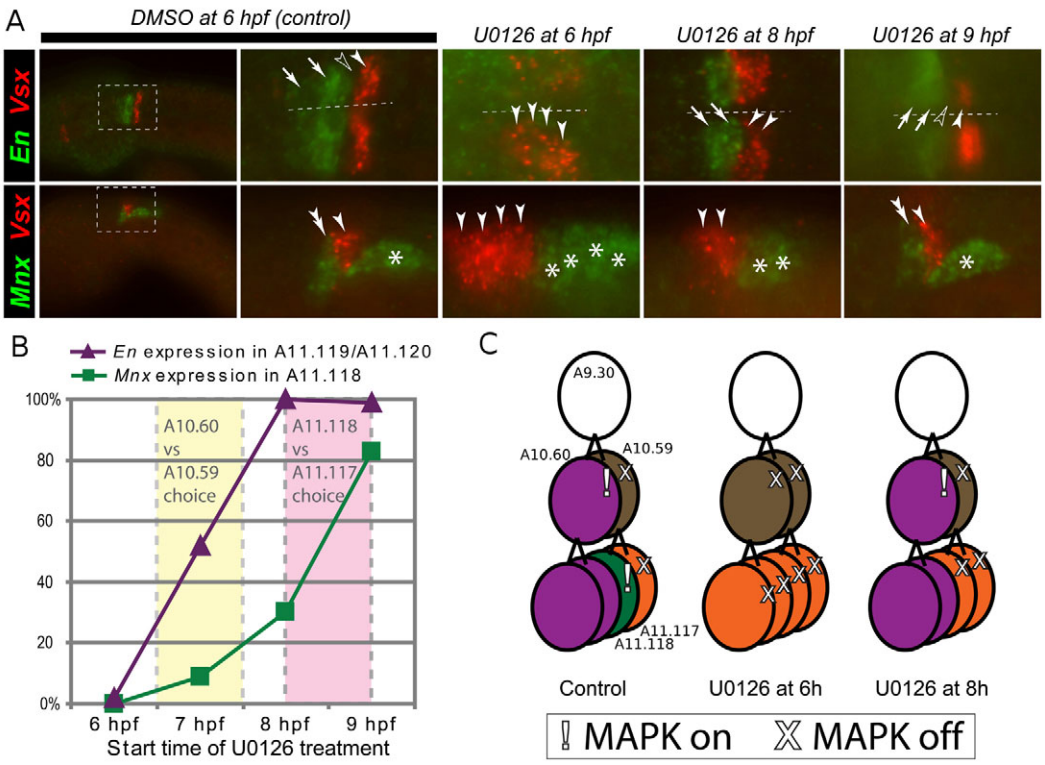

Fig. 2. Treatment with U0126 reveals MAPK-dependent cell fate choices. (**A**) Top: In control *Ciona* embryos, *En* (green) is normally expressed in A11.120 and A11.119 (arrows), whereas *Vsx* is expressed in A11.117 (arrowheads). The gap between *En* and *Vsx* expression represents A11.118 (unfilled arrowheads). Treatment with U0126 at 6 hpf results in loss of *En* and ectopic *Vsx* in all four descendants of A9.30. U0126 at 8 hpf does not abolish *En*, but ectopic *Vsx* is still seen in A11.118. U0126 at 9 hpf does not alter *En* or *Vsx* expression. Bottom: *Mnx* is normally expressed in A11.118 (double arrowhead) and in a motoneuron from the A9.29 lineage (A10.57, asterisk). U0126 at 6 and 8 hpf results in loss of *Mnx* from A11.118 and expansion of *Mnx* in the A9.29 lineage (asterisks). U0126 at 9 hpf does not alter *Mnx* expression. All embryos fixed at 10 hpf. Dashed lines indicate midline. (**B**) Fraction of embryos showing *En* and *Mnx* expression plotted against start time of U0126 treatment. Yellow area represents deduced time window for A10.60 versus A10.59 fate choice. Pink area represents window for A11.118 versus A11.117 fate choice. *n*=50-100 for each time point per assay. (**C**) Model of MAPK signaling events in control embryos or embryos treated with U0126 at 6 hpf or 8 hpf. Colors correspond to cell identity as determined by *En* (purple), *Mnx* (green) or *Vsx* (orange) expression.

of the A11.118 motoneuron into a duplicated A11.117 interneuron) (Fig. 2A-C). This result suggests that the initial specification of the A10.60 and A10.59 progenitor cells is normal, but there is a conversion of A11.118 into an A11.117 fate. Treatment at 9 hpf does not alter expression of *En*, *Vsx* nor *Mnx*. Together, the preceding results suggest that differential MAPK activity is first required for the delineation of the A10.60 and A10.59 fates, and subsequently required for distinguishing A11.118 and A11.117 subtypes. As U0126 is an irreversible inhibitor, treatment at 6 hpf affects both fate choices, resulting in four A11.117-like cells (Fig. 2B,C). Consistent with these observations, di-phosphorylated MAPK (dpMAPK) can be detected in A10.60 and A11.118 of wild-type embryos (supplementary material Fig. S1). Interestingly, *Mnx* expression is expanded within the A9.29 lineage upon U0126 treatment (Fig. 2A). It is normally restricted to the A10.57 motoneuron, the posterior daughter cell of A9.29. Thus, the specification of the A10.57 motoneuron might also depend on differential regulation of MAPK activity.

Ephrin is the positional cue for differential FGF signaling in the MG

Ephrins have been shown to mediate inhibition of FGF/MAPK in the *Ciona* embryo (Picco et al., 2007; Shi and Levine, 2008). Ephrins are membrane-anchored ligands that interact with Eph receptor tyrosine kinases. Ephrin/Eph signaling suppresses MAPK in receiving cells, inhibiting FGF- and MAPK-dependent processes. This has been shown to act at the level of Ras, downstream of the FGF receptor but upstream of MAPK (Elowe et al., 2001; Miao et al., 2001). EphrinAb is expressed in A9.29, which is situated just posterior to A9.30 (Fig. 3A) (Hudson et al., 2007). Thus, EphrinAb+ A9.29 descendants continuously contact the posterior-most cell of the A9.30 lineage. As such, EphrinAb is a strong candidate for the positional cue for MAPK inhibition in A10.59 and A11.117.

To determine whether Ephrin is essential for differential MAPK activity in the A9.30 lineage, a truncated form of the Eph3 receptor that sequesters Ephrin ligand was selectively expressed in this lineage using *FGF8/17/18* regulatory sequences (*FGF8/17/18>Eph3ΔC*) (Picco et al., 2007). The entire lineage is converted to *En*-expressing cells, suggesting ectopic activation of MAPK+ and the transformation of A10.59 into A10.60 (Fig. 3B-D). By contrast, ectopic activation of Ephrin-Eph signaling (via a constitutively activated form of Eph3) abolishes *En* expression, suggesting the reciprocal transformation: A10.60 into A10.59 (supplementary material Fig. S2B). Similarly, treatment of *FGF8/17/18>Eph3ΔC*-electroporated embryos with U0126 also abolishes *En* expression (supplementary material Fig. S2C), confirming that Ephrin signaling acts upstream of, and antagonistic to, MAPK to control cell fate choice.

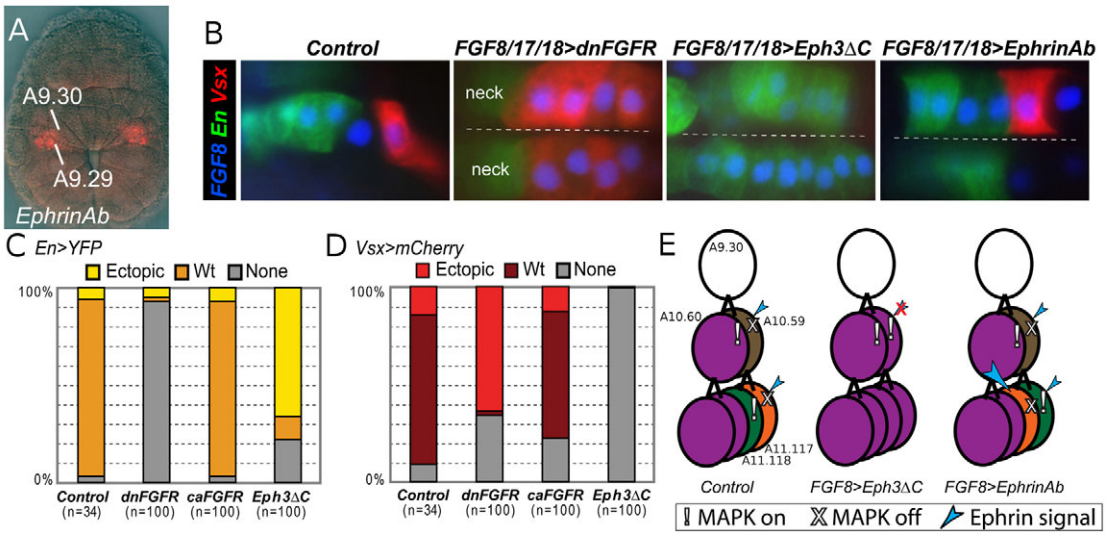

Fig. 3. Ephrin/Eph signaling is the positional cue for MAPK-dependent fate choices. (**A**) *EphrinAb* expression (red) in the A9.29 blastomeres of a late gastrula *Ciona* embryo. (**B**) Embryos co-electroporated with *FGF8/17/18*, *En* and *Vsx* reporters. Co-electroporation of *FGF8/17/18>dnFGFR* results in loss of *En* reporter and expansion of *Vsx* reporter. Note *En* expression in the neck, which lies outside the A9.30 lineage. By contrast, *FGF8/17/18>Eph3ΔC* results in expansion of *En* and loss of *Vsx* reporters. Overexpression of EphrinAb results in *Vsx* expression in A11.118, but not A11.117, indicating a fate 'swap' between these two cells (n=52/100). Dashed line indicates midline. Embryos fixed at 15.5 hpf, 16°C. (**C**) Fractions of embryos in B showing ectopic (yellow), wild-type (orange) or no (gray) *En* reporter expression. Ectopic expression was defined as any expression in the posterior MG (A11.118/A11.117), whereas 'wild-type' expression is only in the anterior (descendants of A11.120/A11.119). Overexpression of a constitutively active form of FGFR (caFGFR) has no effect, as predicted by the model (supplementary material Fig. S3). (**D**) As in C, but scoring for ectopic (red), wild-type (maroon), or no (gray) *Vsx* reporter expression. Ectopic expression was defined as expression in any cell other than A11.117, and 'wild type' is expression only in A11.117. (**E**) Model incorporating Ephrin-dependent downregulation of MAPK in control or perturbation conditions. Colors correspond to cell identity as determined by *En* (purple), *Mnx* (green) or *Vsx* (orange) expression. Large blue arrowhead indicates overexpression of EphrinAb in A9.30 lineage, which can signal to A11.118 and result in preferential MAPK attenuation in this cell in relation to its sister cell.

Ectopic expression of EphrinAb (via *FGF8/17/18>EphrinAb*) inverts the position of A11.117 and A11.118 fates (Fig. 3B,E). Under this condition, the dividing A10.59 cell encounters higher levels of EphrinAb from its anterior A10.60 sister cell. According to the model of Ephrin-MAPK antagonism, this is expected to result in an inversion of A11.118/A11.117 asymmetric MAPK activation and cell fate (explained in supplementary material Fig. S3). Furthermore, the first fate choice (A10.60 versus A10.59) is not affected because Ephrin cannot downregulate MAPK in cis. Overexpression of the other four *Ciona* EphrinA ligands did not cause this phenotype (data not shown). The preceding results suggest that EphrinAb in the A9.29 lineage is the positional cue that inhibits MAPK in A10.59 and A11.117.

Notch signaling regulates the fate choice between A11.120 and A11.119

The first indication of a role for Delta/Notch signaling in patterning the anterior half of the MG came from targeted inhibition of Notch using a dominant-negative form of Su(H) [*FGF8/17/18>Su(H)-DBM*]. These embryos exhibit a duplication of the A12.239 neuron, shown by OFF-ON-OFF-ON expression of *Dmbx*, *PouIV* and *Lhx1/5* in the A10.60 lineage (Fig. 4A; supplementary material Fig. S4A) (Stolfi and Levine, 2011). Similar results are obtained with the γ-secretase inhibitor DAPT, which inhibits proteolytic cleavage of activated Notch receptors (supplementary material Fig. S4B). The duplication of A12.239 identity appears to result from the conversion of A11.119 into an A11.120-like progenitor upon inhibition of Notch signaling (Fig. 4B).

Further evidence for this fate transformation (A11.119 into an ectopic A11.120 progenitor cell) was obtained by visualizing the expression of *Pax3/7*, a key marker of A11.120 and its descendants (Fig. 4C). *Pax3/7* is initially expressed in A11.120, and subsequently in the daughter cells of A11.120, with enhanced expression in A12.239 (posterior daughter cell of A11.120). *Pax3/7* expression is not normally detected in A11.119 or its descendants. However, in embryos electroporated with *FGF8/17/18>Su(H)-DBM* (inhibition of Notch signaling), *Pax3/7* expression is expanded into the A11.119 lineage (Fig. 4C). Further evidence for the transformation of A11.119 into a duplicated A11.120 progenitor cell was obtained by investigating the expression of marker genes for A11.119, including *SoxB1*, *Pax6* and *HesB*. These markers are lost upon targeted inhibition of Notch signaling via *FGF8/17/18>Su(H)-DBM* (supplementary material Fig. S4C). By contrast, there was only a modest reduction of *Nkx6* expression in A11.119, suggesting that it might lie downstream of A11.119 specification (supplementary material Fig. S4C).

We next sought to identify a ligand that could activate Notch in A11.119. *Delta2* is selectively transcribed in A10.59 and its descendants, A11.118 and A11.117 (Fig. 4D,E). *Delta2* expression is also seen later in A11.120 (Fig. 4E). Perhaps Delta2 ligand on the surface of A11.118 activates Notch in the neighboring A11.119 cell. By contrast, A11.120 is not in contact with a Delta2+ cell and, according to the model of lateral inhibition, initiates *Delta2* expression (Doe and Goodman, 1985; Fortini, 2009).

To determine whether *Delta2* expression in the posterior MG (e.g. A10.59) is required for Notch activation in A11.119, we blocked A10.59 specification by transformation with the

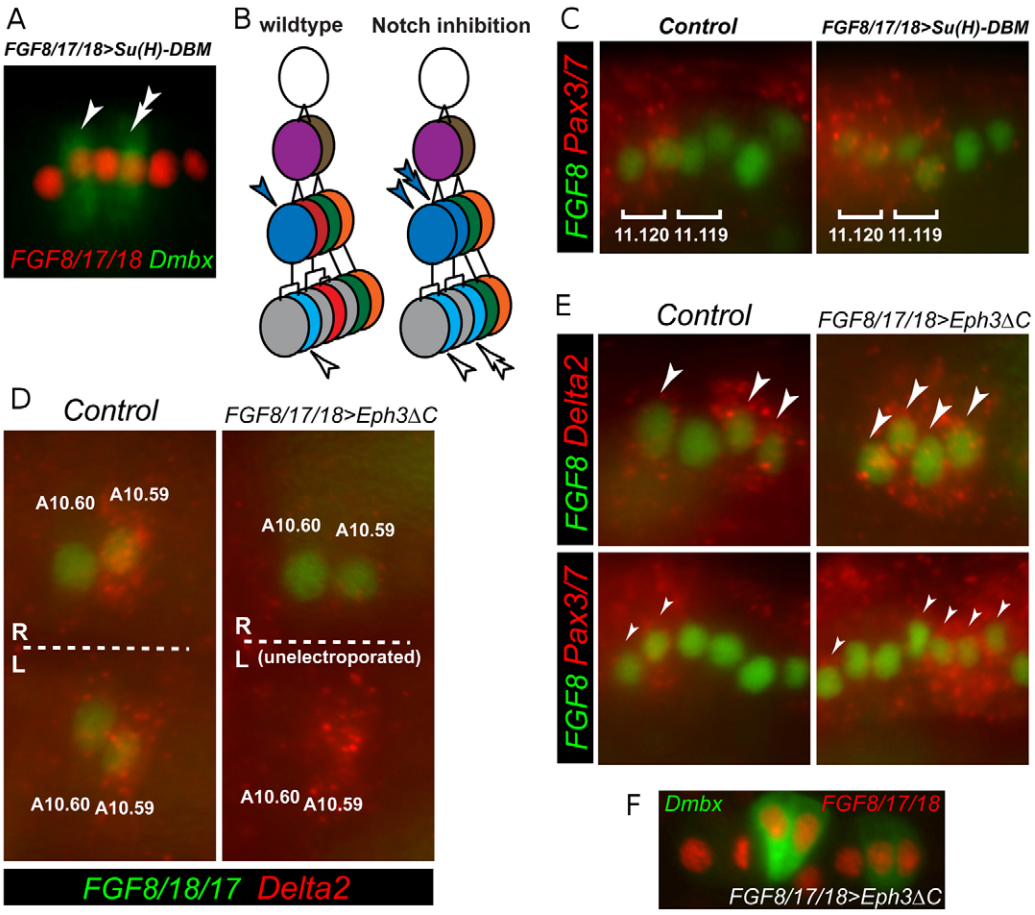

Fig. 4. Notch signaling is required for specification of A11.119 in *Ciona*. (**A**) Ectopic expression of A12.239 marker *Dmbx* in posterior daughter cell of A11.119 (A12.237, double arrowhead) upon inhibition of Notch signaling by *FGF8/17/18>Su(H)-DBM* (*n*=66/100). Single arrowhead indicates A12.239 cell. (**B**) Model according to results shown in A. Colors correspond to the following cell identities: A9.30 (white), A10.60 (purple), A10.59 (brown), A11.120 (dark blue), A11.119 (dark red), A11.118 (green), A11.117 (orange), A12.239 (light blue), A13.474 (light red) and ependymal cells (gray). Ectopic expression of A12.239 markers is interpreted as a duplication of A11.120 fate (dark blue) at the expense of A11.119 (dark red), resulting in two A12.239-like neurons one cell division later (light blue). 'Original' cells indicated by single arrowheads, double arrowheads indicate corresponding ectopic duplicate cells. (**C**) *Pax3/7* is normally expressed in A11.120. *FGF8/17/18>Su(H)-DBM* results in expansion of *Pax3/7* expression into A11.119 descendants (*n*=68/100). (**D**) *Delta2* is normally expressed in A10.59 pair. Weaker/transient expression is sometimes seen in A10.60 (control embryo, left side), but it is never equal to that of A10.59. Conversion of A10.59 to A10.60 fate with *FGF8/17/18>Eph3ΔC* results in loss of *Delta2* expression in A10.59 in electroporated side but not in unelectroporated side (*n*=74/95). Dashed lines indicate embryo midlines. R, right side; L, left side. Embryos fixed at 8 hpf, 20°C. (**E**) Top panels: Later *Delta2* expression under same conditions as in D. Ectopic *Delta2* expression is seen in A11.119 upon loss of A10.59 fate (*n*=56/71) and is interpreted as loss of Notch activation in A11.119 according to the model of lateral inhibition. Bottom panels: altered *Pax3/7* expression in the next mitotic generation, under same conditions (*n*=44/54). Arrowheads denote *Pax3/7*- or *Delta2*-expressing cells. (**F**) *FGF8/17/18>Eph3ΔC* results in abnormal *Dmbx* reporter expression, as a result of de-regulation of Delta/Notch signaling and *Pax3/7*. A9.30 lineage tracing in all panels was performed using *FGF8/17/18* ('*FGF8*') reporter plasmid. All *Pax3/7* in situ hybridizations performed on embryos fixed at 12.5 hpf, 16°C.

FGF8/17/18>Eph3ΔC transgene (constitutive MAPK activation in A10.60 and A10.59). Early *Delta2* expression in A10.59 is lost (Fig. 4D) and *Delta2* is ectopically expressed in A11.119 (Fig. 4E). As a result, *Pax3/7* and *Dmbx* are de-regulated, as the cells are left to resolve their Notch signaling status through lateral inhibition without the positional cue normally provided by A10.59/A11.118 (Fig. 4E,F). If Notch signaling is inhibited in this background by co-electroporation with *FGF8/17/18>Su(H)-DBM*, all cells of the lineage activate *Dmbx*, as expected (supplementary material Fig. S4D).

To test whether Delta2 is sufficient to impinge on A11.119/A11.120 fate, we mis-expressed it using the *En* driver (*En>Delta2*). *En* expression is initiated in both daughter cells of A10.60, but is strongly upregulated in A11.119 and downregulated in A11.120. Electroporation of *En>Delta2* results in a proportion of embryos showing inverted expression of *Pax3/7*, suggesting a conversion of A11.120 into A11.119 and vice versa (supplementary material Fig. S4E). As a result, *Dmbx* reporter expression is similarly altered (supplementary material Fig. S4F). Taken together, these results suggest that a Delta2-mediated relay from the posterior MG patterns the anterior MG; *Delta2* expression in the posterior A9.30 lineage is dependent on the inhibition of FGF signaling by localized EphrinAb (supplementary material Fig. S5).

Pax3/7 activates Dmbx in A12.239

We hypothesized that the localized expression of *Pax3/7* in A11.120 might be required for specification of its daughter cell A12.239, as ectopic expression of *Pax3/7* in A11.119 correlates

with ectopic activation of marker genes normally expressed in A12.239: *Lhx1/5*, *PouIV* and *Dmbx*. Moreover, inhibition of Pax3/7 via morpholino injection results in loss of *PouIV* and *Lhx1/5* expression (Imai et al., 2009). Thus, it would appear that *Lhx1/5*, *PouIV* and *Dmbx* are directly or indirectly co-regulated by *Pax3/7*.

This was tested by mis-expression of Pax3/7 throughout the A9.30 lineage with the *FGF8/17/18* driver (*FGF8/17/18>Pax3/7*). The resulting embryos exhibit ectopic expression of the *Dmbx>GFP* reporter gene throughout the A9.30 lineage (Fig. 5A). Strikingly, the mis-expression of Pax3/7 also results in the formation of supernumerary decussating neurons (Fig. 5B). Similar results were obtained with a heterologous Pax3/7::VP16 transcriptional activator (data not shown), whereas a repressor form of Pax3/7 (Pax3/7::WRPW) strongly represses *Dmbx* (Fig. 5A). Thus, Pax3/7 appears to function as an activator that either directly or indirectly activates *Dmbx* expression in A12.239.

To determine whether Pax3/7 directly activates *Dmbx*, we analyzed the sequence of a minimal ~300 bp enhancer from the *Dmbx* 5′ regulatory region that is sufficient to mediate low levels of restricted expression in the A12.239 decussating neuron (Fig. 5D). A putative Pax3 binding site (Lagha et al., 2008) was identified within this minimal enhancer (Fig. 5C). Mutation of this site abolishes the activity of the enhancer (Fig. 5D). The Pax3/7 binding site is also conserved in the related species *C. savignyi* and is essential for the activity of the *C. savignyi* minimal enhancer in transgenic *C. intestinalis* embryos (Fig. 5E).

The preceding results suggest that Pax3/7 directly activates *Dmbx* expression in the A12.239 neuron. Additional evidence was obtained by in vitro binding assays. Gel shift assays were performed with recombinant *Ciona* Pax3/7 protein and double-stranded DNA oligonucleotides containing either the normal or mutant version of the Pax3/7 binding motif in the presence of a 1500-fold mass excess of the nonspecific competitor poly dI-dC. Under these conditions, Pax3/7 exhibited a 3.5-fold increase in binding to the wild-type motif compared with the mutant motif (Fig. 5F). This appears modest when contrasted with the dramatic effect the mutation has on the minimal *Dmbx* enhancer in vivo. However, mutation of the Pax3/7 site within the context of the 'full-length' *Dmbx* enhancer results in a similarly moderate decrease in activity (expression seen in 12/100 mutant versus 52/100 wild type; data not shown), suggesting that the minimal enhancer is particularly sensitized to binding site mutations. We conclude that Pax3/7 directly activates *Dmbx* expression.

Pax3/7 is also expressed in additional cell types, most conspicuously in neural plate border cells (supplementary material Fig. S6A). We hypothesized Pax3/7 is cooperating with the

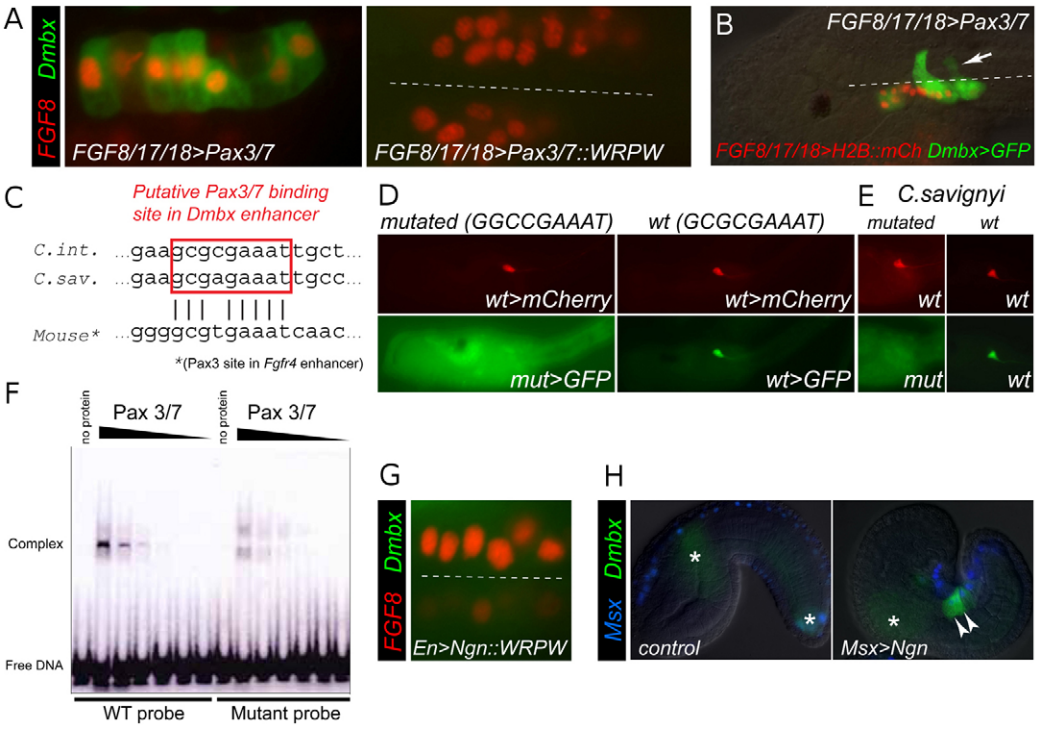

Fig. 5. Pax3/7 as a direct transcriptional activator of *Dmbx*. (**A**) Pax3/7 mis-expression activates ectopic *Dmbx* reporter expression (left, *n*=76/100). Overexpression of Pax3/7::WRPW completely abolishes *Dmbx* reporter (right, *n*=100/100). *Ciona* embryos fixed at 15.5 hpf at 16°C. (**B**) Ectopic *Dmbx*+ neurons generated by Pax3/7 mis-expression project contralaterally (*n*=35/100). Nascent axon indicated by arrow. Embryos fixed at 17.5 hpf at 16°C. (**C**) Alignment of putative Pax3/7 binding sites in minimal *Dmbx* enhancers from *C. intestinalis* and *C. savignyi*, and with the 'P4' Pax3 binding site from a mouse *Fgfr4* enhancer (Lagha et al., 2008). (**D**) Larvae co-electroporated with wild-type and/or mutated minimal *Dmbx* reporter constructs. Mutation of the predicted Pax3/7 site abolishes reporter activity (bottom left, GFP expression seen in only 1/100 embryos). Activity of co-electroporated wild-type reporter (distinguished by *mCherry*) is not affected (top left panel). Compare with co-electroporation of both *GFP* and *mCherry* wild-type reporters (right panels). (**E**) Co-electroporation of reporters using the minimal *Dmbx* enhancer from *C. savignyi* in *C. intestinalis* larvae. Disruption of the conserved Pax3/7 binding site abolishes expression (*n*=19/21). (**F**) EMSA of purified recombinant Pax3/7 and wild-type and mutant Pax3/7 binding motif-containing oligonucleotides in the presence of a nonspecific competitor. Pax3/7 preferentially binds the wild-type motif. (**G**) *En>Ngn::WRPW* abolishes *Dmbx* reporter (*n*=97/100). Embryo fixed at 15.5 hpf at 16°C. (**H**) Mis-expression of Ngn in Pax3/7+ neural plate borders using the *Msx* driver results in ectopic *Dmbx* reporter expression (arrowheads, *n*=92/100). Asterisks indicate leaky *Dmbx* reporter expression in mesoderm. A9.30 lineage tracing performed using *FGF8/17/18* ('*FGF8*') reporter plasmid. Dashed lines indicate midline.

neurogenic bHLH factor Neurogenin (Ngn) to activate *Dmbx* in the MG. *Ngn* is transiently expressed in MG precursors and is maintained in A12.239 (supplementary material Fig. S6B,C) Expression of a repressor form of Ngn (Ngn::WRPW) abolishes *Dmbx* expression (Fig. 5G). Furthermore, mis-expression of Ngn in the neural plate border, where Pax3/7 is normally present, is sufficient to activate *Dmbx* in these cells (Fig. 5H). Thus, Ngn and Pax3/7 cooperatively activate *Dmbx* and specify an A12.239 decussating MG interneuron fate.

Inhibition of MAPK promotes specification of A12.239

The preceding results suggest that Pax3/7 expression in A11.120 activates *Dmbx* (and perhaps additional makers) in A12.239 (posterior daughter cell of A11.1120) but not A12.240 (anterior daughter cell of A11.120). What inhibits *Dmbx* expression in A12.240? We reasoned that this was linked to the choice between neuronal and non-neuronal fate. In contrast to the A12.239 neuron, A12.240 is an undifferentiated cell that expresses the neural progenitor marker *SoxB1* and gives rise to four ependymal cells (i.e. quiescent stem cells) (Horie et al., 2011).

Delta/Notch-mediated lateral inhibition is frequently invoked as a determinant of neuron/non-neuron cell fate decisions (Fortini, 2009; Pierfelice et al., 2011). Downregulation of Notch signaling in the anterior MG results in occasional 'twin' neurons. That is, both A12.240 and A12.239 undergo neurogenesis and express *Dmbx*. However, this effect is not enhanced by increasing levels of Notch inhibition (Fig. 6E; supplementary material Fig. S7). We thereby sought to identify other signaling processes that might influence the asymmetric fates of A11.120 daughter cells.

Involvement of MAPK in distinguishing A12.240 from A12.239 was suggested by immunostaining for dpMAPK, which revealed MAPK activation in A12.240 but not A12.239 (Fig. 6A,B). FGF/MAPK is known to inhibit neural differentiation in vertebrates (del Corral et al., 2002; Mathis et al., 2001). We hypothesized that FGF/MAPK signaling is required for *SoxB1* expression and repression of neurogenesis in A12.240. To test this idea, FGF/MAPK signaling was perturbed by late addition of the MEK inhibitor U0126, in order to avoid disruption of earlier MAPK-dependent patterning (Fig. 6C,D). *SoxB1* expression is abolished in A12.240 (Fig. 6C) and there is ectopic activation of *Dmbx*,

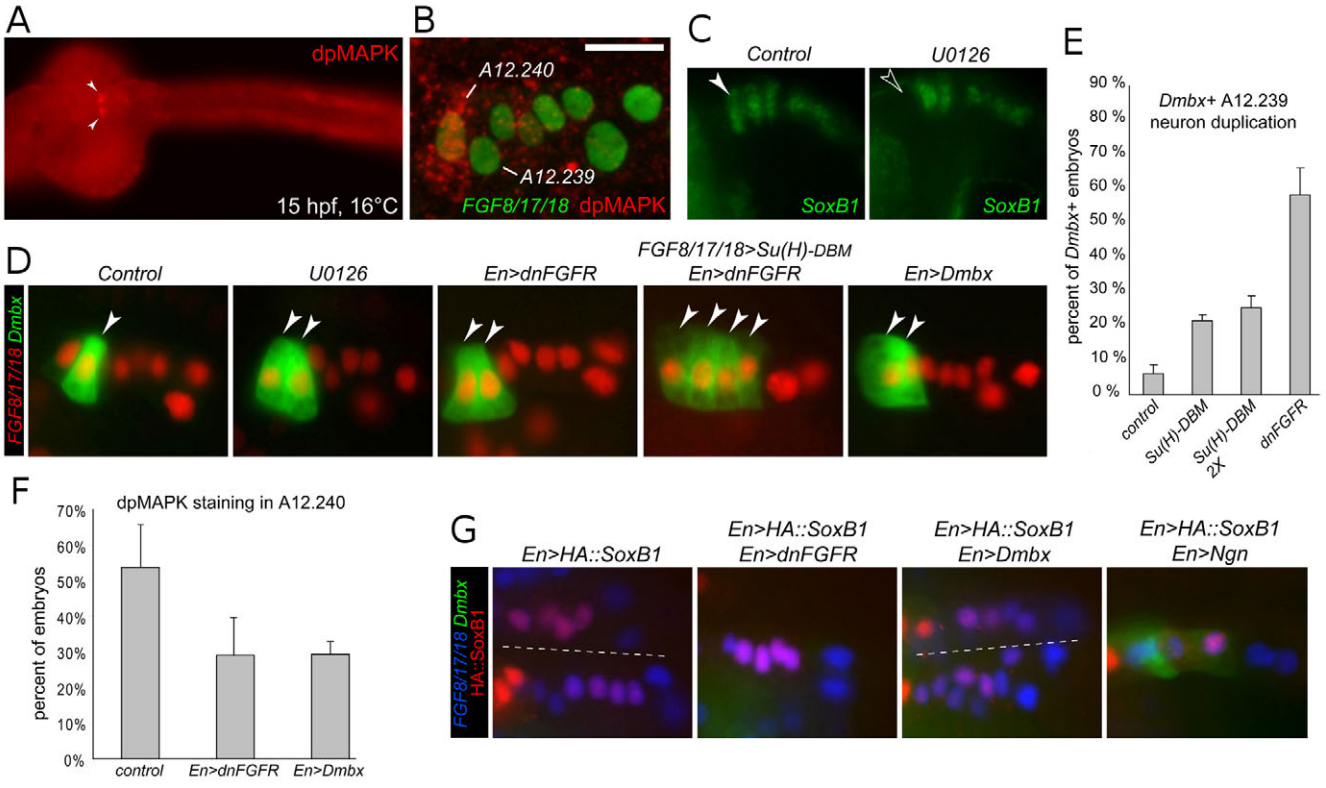

Fig. 6. Involvement of FGF/MAPK, Dmbx and SoxB1 in A12.240 versus A12.239 cell fate decision. (**A**) Immunohistochemistry for dpMAPK in A12.240 cell pair (arrowheads). (**B**) *FGF8/17/18* reporter (green) and dpMAPK (red) double staining shows pronounced MAPK activation in A12.240 relative to its sister cell, A12.239. (**C**) In control *Ciona* embryos, *SoxB1* expression is seen in three non-neuronal cells of the MG, including A12.240 (filled arrowhead). Late U0126 treatment (11 hpf) abolishes *SoxB1* in A12.240 (unfilled arrowhead, *n*=36/45). Embryos fixed 14.5 hpf, 16°C. (**D**) In control embryos, *Dmbx* reporter is expressed in A12.239. Late U0126 treatment results in 'twinning' of *Dmbx*+ neurons (arrowheads) (*n*=74/100). Twinning is also achieved with *En>dnFGFR* (*n*=52/100). Combining both early Notch and late FGF perturbation [*FGF8/17/18>Su(H)-DBM* + *En>dnFGFR*] results in four *Dmbx*+ cells (two sets of 'twins', *n*=58/100). Electroporation of *En>Dmbx* also results in 'twinning' of A12.239 (*n*=117/172). Embryos fixed 15.5-17.5 hpf, 16°C. (**E**) Quantification of 'twinning' phenotype in conditions of Notch [*En>Su(H)-DBM*] or FGF [*En>dnFGFR*] inhibition, averaged over three replicates (*n*=100/replicate). Error bars indicate s.d. (**F**) Quantification of dpMAPK staining in A12.240 in embryos electroporated with *En>dnFGFR* or *En>Dmbx* compared with control embryos, averaged over three replicates (*n*=100/replicate). Error bars indicate s.d. Embryos fixed at 15.75 hpf, 16°C. (**G**) SoxB1 overexpression abolishes *Dmbx* reporter expression (*n*=82/100), overriding the 'twinning' phenotype of *En>dnFGFR* (*n*=91/100) or *En>Dmbx* (*n*=86/100). *Dmbx* reporter expression is partially rescued by co-electroporation of *En>Ngn* (*n*=45/100). Embryos fixed 15.5 hpf, 16°C. Dashed line indicates midline.

resulting in twin neurons (Fig. 6D). Axonal projections from these 'twins' are often impaired, although they still extend contralaterally. The ectopic decussating neuron sometimes projects its axon anteriorly instead of towards the tail (supplementary material Fig. S8).

This twinning phenotype was mimicked by targeted expression of dnFGFR using the *En* driver (Fig. 6D). Moreover, combined inhibition of both FGF signaling (*En>dnFGFR*) and Notch signaling [*FGF8/17/18>Su(H)-DBM*] results in the transformation of all four descendants of A10.60 into Dmbx+ decussating neurons (Fig. 6D). In these experiments, inhibition of Notch signaling results in the transformation of A11.119 into A11.120, and both sets of daughter cells lack MAPK activation and express *Dmbx*. These results suggest that FGF-MAPK signaling inhibits neurogenesis in A12.240 as well as in ectopic A12.240-like cells.

Mis-expression of Dmbx using the *En* driver unexpectedly recapitulated the twinning phenotype (Fig. 6D). Upon electroporation with either *En>dnFGFR* or *En>Dmbx*, there is a loss of dpMAPK staining in A12.240 (Fig. 6F). Dmbx1 is thought to act as a repressor in vertebrates, and we found that a repressor form of Dmbx (Dmbx::WRPW) recapitulates the activity of the full-length protein (n=51/69, data not shown). Thus, we hypothesize that Dmbx can promote its own expression by repressing FGF/MAPK signaling.

In vertebrates, SoxB1 genes promote a neural progenitor identity but can inhibit neuronal differentiation by interfering with proneural gene activity (Bylund et al., 2003; Graham et al., 2003; Holmberg et al., 2008). To test the role of SoxB1, we overexpressed it using the *En* driver (Fig. 6G). This results in loss of *Dmbx* reporter expression, consistent with the conversion of A12.239 to A12.240. Electroporation of *En>SoxB1* also overrides the 'twinning' phenotype of *En>dnFGFR* or *En>Dmbx*. Co-electroporation with *En>Ngn* partially rescues *Dmbx* expression, suggesting that SoxB1 might function downstream of FGF signaling to inhibit Ngn activity.

It is conceivable that Delta/Notch signaling itself contributes to asymmetric activation of MAPK in A11.120 daughter cells. First, we observed a moderate 'twinning' effect upon Notch inhibition (Fig. 6E; supplementary material Fig. S7). Second, Delta/Notch lateral inhibition effectors *Ngn* and *HesB* show mutually exclusive expression patterns, which is consistent with the lateral inhibition model: *Ngn* is expressed in A12.239, whereas *HesB* is expressed in A12.240 (supplementary material Fig. S6B). Delta/Notch signaling could bias Ngn and Pax3/7 expression to A12.239. Ngn and Pax3/7 cooperatively activate Dmbx, which, in turn, downregulates MAPK activity, thereby repressing SoxB1 expression and promoting cell-cycle exit. Thus, we propose that a Notch-FGF relay, mediated by Dmbx, is operating to determine asymmetric neuronal differentiation (summarized in Fig. 7B).

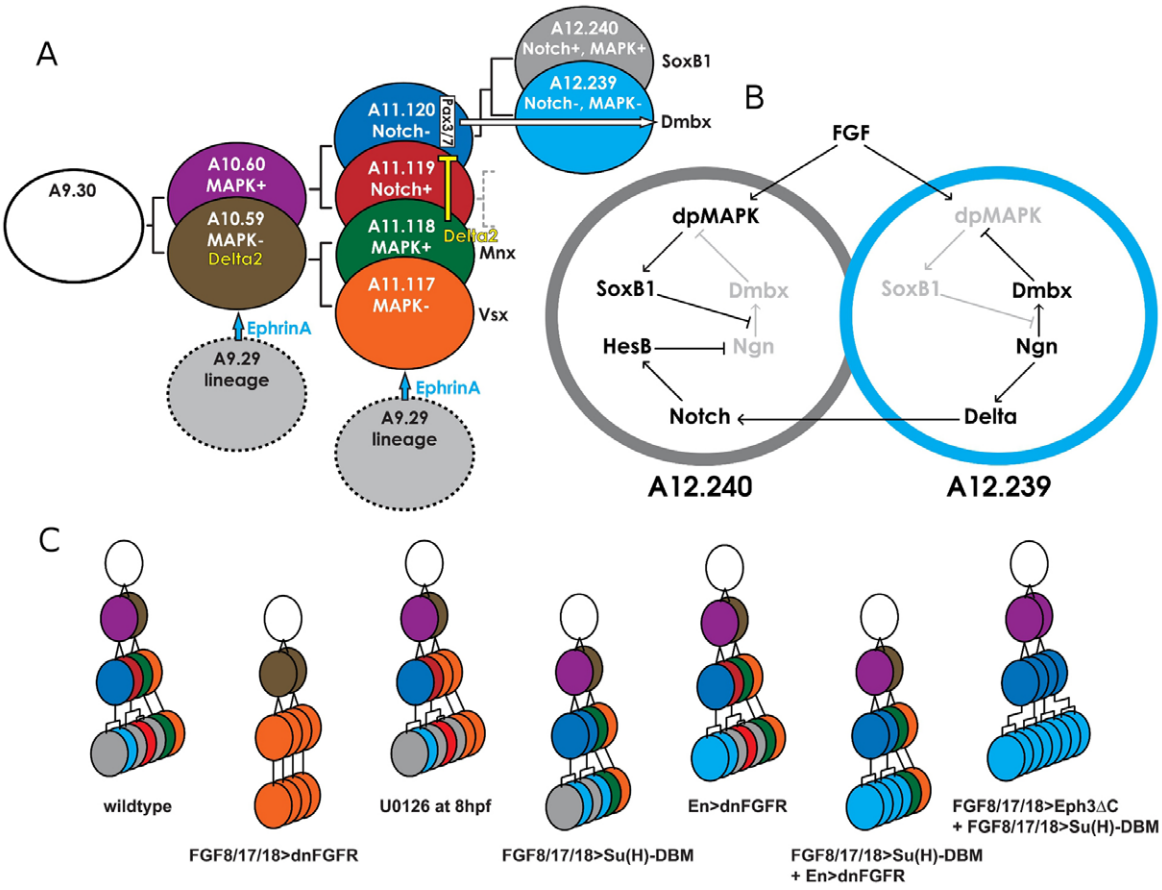

Fig. 7. Summary diagrams. (**A**) Summary of cell signaling events and transcriptional regulation setting up the specification and differentiation of A12.239. Anterior is at the top, posterior is at the bottom. (**B**) Diagram of FGF-SoxB1-Dmbx interactions operating in the context of A12.240 and A12.239. FGF/MAPK signaling is required for expression of SoxB1, which can inhibit activation of Dmbx by Ngn. Ngn feeds into the Delta/Notch pathway and Dmbx can downregulate FGF/MAPK activity. Thus, Dmbx could function to integrate these two pathways (see text for details). (**C**) Summary of different MG neuron configurations resulting from various perturbation conditions described in this study. Colors correspond to the following cell identities: A9.30 (white), A10.60 (purple), A10.59 (brown), A11.120 (dark blue), A11.119 (dark red), A11.118 (green), A11.117 (orange), A12.239 (light blue), A13.474 (light red) and ependymal cells (gray).

DISCUSSION

We have presented evidence that the specification of *Ciona* MG neuronal subtypes depends on short-range Ephrin, FGF and Delta/Notch signals. The A9.30 blastomere expresses FGF8/17/18, which serves as an intrinsic source of FGF signaling within the lineage (Imai et al., 2009). Differential MAPK activity within the A9.30 lineage depends on EphrinAb in the neighboring A9.29 lineage (summarized in Fig. 7A). Inhibition of MAPK in the posterior A10.59 cell leads to expression of a Delta2 ligand. This, in turn, triggers Notch signaling in the posterior daughter of A10.60 (A11.119). The activation of Notch signaling in A11.119 restricts the expression of Pax3/7 to the anterior-most cell of the lineage, A11.120. Pax3/7 appears to be a direct activator of *Dmbx* expression in the posterior daughter of A11.120 (A12.239). Differential Notch and MAPK activity in the A11.120 daughter cells promotes *Dmbx* expression and neurogenesis in A12.239 ($Notch^{OFF}$, $MAPK^{OFF}$), and SoxB1 expression and maintenance of the progenitor state in A12.240 ($Notch^{ON}$, $MAPK^{ON}$). Perturbation of different components of these pathways at different times and in different cells results in tadpoles with altered configurations of MG neurons (Fig. 7C).

Delta/Notch signaling, propagated by lateral inhibition, could be providing the spatial cue for differential MAPK+ activity in the A12.240 and A12.239 sister cells. It is possible that A12.240 experiences Notch signaling leading to restricted expression of Ngn in A12.239, and localized activation of *Dmbx* by the combination of Ngn and Pax3/7. Dmbx somehow inhibits MAPK activity, thereby repressing *SoxB1* expression in A12.239 and promoting differentiation (Fig. 7B). In zebrafish, Dmbx1a has been shown to promote cell-cycle exit and differentiation of neurons (Wong et al., 2010). It will be interesting to see whether this is occurring in the context of Delta/Notch lateral inhibition and whether it functions to counteract FGF and SoxB1, as seen in the *Ciona* MG.

Comparisons with the vertebrate spinal cord

The patterning of the *Ciona* MG depends on extracellular positional cues that are distinct from those operating in the vertebrate spinal cord. The MG is patterned by a succession of short-range Ephrin, FGF and Delta/Notch signaling, whereas the spinal cord depends on long-range Shh and BMP gradients. Despite these distinct spatial patterning mechanisms, there are similarities in the gene expression profiles of the neuronal progenitors. This is apparent in both the AP-DV correspondence of transcription factor expression profiles as well as the apparent conservation of combinatorial transcriptional codes for motoneurons and interneuron subtypes.

Despite the contrast in short-range versus long-range positional cues between the two systems, certain signaling strategies might be conserved. In the vertebrate spinal cord, downregulation of FGF signaling is required for neurogenesis (del Corral et al., 2002), and Notch has been shown to regulate neuronal subtype diversification (Peng et al., 2007), suggesting that FGF and Notch signaling could be used for short-range 'fine-tuning' of cell fates within broad DV patterning domains. Furthermore, retinoic acid (RA)-dependent *Hox1* expression in both the *Ciona* anterior MG (Imai et al., 2009; Nagatomo and Fujiwara, 2003) and the vertebrate hindbrain (Marshall et al., 1992) raises the intriguing possibility that ascidians have consolidated DV and AP patterning of the CNS along a single axis.

Beyond the mechanisms underlying patterning and cell fate choice, the *Ciona* MG and vertebrate spinal cord might share gene regulatory networks controlling axon guidance and neuronal connectivity. We have shown that Pax3/7 regulates the expression of *Dmbx* and *Lhx1/5* expression in A12.239 and is sufficient to impose a contralateral projection when mis-expressed in other MG neurons. In vertebrates, *Pax3* and *Pax7* are required for ventral commissure formation in the spinal cord (Mansouri and Gruss, 1998). *Lhx1/5* is a known marker of commissural dorsal spinal cord interneurons (Gowan et al., 2001; Reeber et al., 2008), though it remains to be seen whether *Dmbx1*+ spinal cord neurons are also decussating (Gogoi et al., 2002; Ohtoshi and Behringer, 2004). Thus, ascidians and vertebrates might share a conserved *Pax3/7*-dependent regulatory network to specify a decussating interneuron identity.

Acknowledgements

We thank N. Kam, O. Hobert, S. Amacher, J. Gerhart, L. Feldman and members of the Levine laboratory for comments; and W. Shi for sharing Eph3ΔC and Eph4ΔC constructs.

Funding

This study was supported by funds from the Francis Williams Chair in Genetics to M.L., and by an Achievement Rewards for College Scientists (ARCS) Foundation graduate student fellowship to A.S.

Competing interests statement

The authors declare no competing financial interests.

Supplementary material

Supplementary material available online at
http://dev.biologists.org/lookup/suppl/doi:10.1242/dev.072108/-/DC1

References

Beh, J., Shi, W., Levine, M., Davidson, B. and Christiaen, L. (2007). FoxF is essential for FGF-induced migration of heart progenitor cells in the ascidian Ciona intestinalis. *Development* **134**, 3297-3305.

Briscoe, J. and Novitch, B. G. (2008). Regulatory pathways linking progenitor patterning, cell fates and neurogenesis in the ventral neural tube. *Philos. Trans. R. Soc. B Biol. Sci.* **363**, 57-70.

Briscoe, J., Sussel, L., Serup, P., Hartigan-O'Connor, D., Jessell, T., Rubenstein, J. and Ericson, J. (1999). Homeobox gene Nkx2. 2 and specification of neuronal identity by graded Sonic hedgehog signalling. *Nature* **398**, 622-626.

Briscoe, J., Pierani, A., Jessell, T. M. and Ericson, J. (2000). A homeodomain protein code specifies progenitor cell identity and neuronal fate in the ventral neural tube. *Cell* **101**, 435-445.

Brown, E. R., Nishino, A., Bone, Q., Meinertzhagen, I. A. and Okamura, Y. (2005). GABAergic synaptic transmission modulates swimming in the ascidian larva. *Eur. J. Neurosci.* **22**, 2541-2548.

Bylund, M., Andersson, E., Novitch, B. G. and Muhr, J. (2003). Vertebrate neurogenesis is counteracted by Sox1-3 activity. *Nat. Neurosci.* **6**, 1162-1168.

Christiaen, L., Wagner, E., Shi, W. and Levine, M. (2009). The sea squirt Ciona intestinalis. *Cold Spring Harbor Protocols* doi:10.1101/pdb.emo138.

Cole, A. G. and Meinertzhagen, I. A. (2004). The central nervous system of the ascidian larva: mitotic history of cells forming the neural tube in late embryonic Ciona intestinalis. *Dev. Biol.* **271**, 239-262.

Davidson, B., Shi, W., Beh, J., Christiaen, L. and Levine, M. (2006). FGF signaling delineates the cardiac progenitor field in the simple chordate, Ciona intestinalis. *Genes Dev.* **20**, 2728-2738.

del Corral, R. D., Breitkreuz, D. N. and Storey, K. G. (2002). Onset of neuronal differentiation is regulated by paraxial mesoderm and requires attenuation of FGF signalling. *Development* **129**, 1681-1691.

Delsuc, F., Brinkmann, H., Chourrout, D. and Philippe, H. (2006). Tunicates and not cephalochordates are the closest living relatives of vertebrates. *Nature* **439**, 965-968.

Doe, C. Q. and Goodman, C. S. (1985). Early events in insect neurogenesis. II. The role of cell interactions and cell lineage in the determination of neuronal precursor cells. *Dev. Biol.* **111**, 206-219.

Elowe, S., Holland, S. J., Kulkarni, S. and Pawson, T. (2001). Downregulation of the Ras-mitogen-activated protein kinase pathway by the EphB2 receptor tyrosine kinase is required for ephrin-induced neurite retraction. *Mol. Cell. Biol.* **21**, 7429-7441.

Ericson, J., Morton, S., Kawakami, A., Roelink, H. and Jessell, T. M. (1996). Two critical periods of Sonic Hedgehog signaling required for the specification of motor neuron identity. *Cell* **87**, 661-673.

Ericson, J., Rashbass, P., Schedl, A., Brenner-Morton, S., Kawakami, A., Van Heyningen, V., Jessell, T. and Briscoe, J. (1997). Pax6 controls progenitor cell identity and neuronal fate in response to graded Shh signaling. *Cell* **90**, 169-180.

Fortini, M. E. (2009). Notch signaling: the core pathway and its posttranslational regulation. *Dev. Cell* **16**, 633-647.

Gogoi, R., Schubert, F., Martinez-Barbera, J., Acampora, D., Simeone, A. and Lumsden, A. (2002). The paired-type homeobox gene Dmbx1 marks the midbrain and pretectum. *Mech. Dev.* **114**, 213-217.
Goulding, M. (2009). Circuits controlling vertebrate locomotion: moving in a new direction. *Nat. Rev. Neurosci.* **10**, 507-518.
Gowan, K., Helms, A. W., Hunsaker, T. L., Collisson, T., Ebert, P. J., Odom, R. and Johnson, J. E. (2001). Crossinhibitory activities of Ngn1 and Math1 allow specification of distinct dorsal interneurons. *Neuron* **31**, 219-232.
Graham, V., Khudyakov, J., Ellis, P. and Pevny, L. (2003). SOX2 functions to maintain neural progenitor identity. *Neuron* **39**, 749-765.
Grave, C. (1921). Amaroucium constellatum (Verrill). 2. The structure and organization of the tadpole larva. *J. Morphol.* **36**, 71-92.
Holmberg, J., Hansson, E., Malewicz, M., Sandberg, M., Perlmann, T., Lendahl, U. and Muhr, J. (2008). SoxB1 transcription factors and Notch signaling use distinct mechanisms to regulate proneural gene function and neural progenitor differentiation. *Development* **135**, 1843-1851.
Horie, T., Nakagawa, M., Sasakura, Y., Kusakabe, T. G. and Tsuda, M. (2010). Simple motor system of the ascidian larva: neuronal complex comprising putative cholinergic and GABAergic/glycinergic neurons. *Zool. Sci.* **27**, 181-190.
Horie, T., Shinki, R., Ogura, Y., Kusakabe, T. G., Satoh, N. and Sasakura, Y. (2011). Ependymal cells of chordate larvae are stem-like cells that form the adult nervous system. *Nature* **469**, 525-528.
Hudson, C. and Yasuo, H. (2006). A signalling relay involving Nodal and Delta ligands acts during secondary notochord induction in Ciona embryos. *Development* **133**, 2855-2864.
Hudson, C., Lotito, S. and Yasuo, H. (2007). Sequential and combinatorial inputs from Nodal, Delta2/Notch and FGF/MEK/ERK signalling pathways establish a grid-like organisation of distinct cell identities in the ascidian neural plate. *Development* **134**, 3527-3537.
Hudson, C., Ba, M., Rouvière, C. and Yasuo, H. (2011). Divergent mechanisms specify chordate motoneurons: evidence from ascidians. *Development* **138**, 1643-1652.
Ikuta, T. and Saiga, H. (2007). Dynamic change in the expression of developmental genes in the ascidian central nervous system: revisit to the tripartite model and the origin of the midbrain-hindbrain boundary region. *Dev. Biol.* **312**, 631-643.
Imai, J. and Meinertzhagen, I. (2007). Neurons of the ascidian larval nervous system in Ciona intestinalis: I. Central nervous system. *J. Comp. Neurol.* **501**, 316-334.
Imai, K., Stolfi, A., Levine, M. and Satou, Y. (2009). Gene regulatory networks underlying the compartmentalization of the Ciona central nervous system. *Development* **136**, 285-293.
Kajiwara, S. and Yoshida, M. (1985). Changes in behavior and ocellar structure during the larval life of solitary ascidians. *Biol. Bull.* **169**, 565-577.
Lagha, M., Kormish, J. D., Rocancourt, D., Manceau, M., Epstein, J. A., Zaret, K. S., Relaix, F. and Buckingham, M. E. (2008). Pax3 regulation of FGF signaling affects the progression of embryonic progenitor cells into the myogenic program. *Genes Dev.* **22**, 1828-1837.
Lee, K. J., Dietrich, P. and Jessell, T. M. (2000). Genetic ablation reveals that the roof plate is essential for dorsal interneuron specification. *Nature* **403**, 734-740.
Lee, S., Lee, B., Joshi, K., Pfaff, S., Lee, J. and Lee, S. (2008). A regulatory network to segregate the identity of neuronal subtypes. *Dev. Cell* **14**, 877-889.
Lemaire, P. (2011). Evolutionary crossroads in developmental biology: the tunicates. *Development* **138**, 2143-2152.
Mackie, G. and Bone, Q. (1976). Skin impulses and locomotion in an ascidian tadpole. *J. Marine Biol. Assoc. UK* **56**, 751-768.
Mansouri, A. and Gruss, P. (1998). Pax3 and Pax7 are expressed in commissural neurons and restrict ventral neuronal identity in the spinal cord. *Mech. Dev.* **78**, 171-178.
Marder, E. and Bucher, D. (2001). Central pattern generators and the control of rhythmic movements. *Curr. Biol.* **11**, R986-R996.
Marshall, H., Nonchev, S., Sham, M. H., Muchamore, I., Lumsden, A. and Krumlauf, R. (1992). Retinoic acid alters hindbrain Hox code and induces transformation of rhombomeres 2/3 into a 4/5 identity. *Nature* **360**, 737-741.
Mathis, L., Kulesa, P. M. and Fraser, S. E. (2001). FGF receptor signalling is required to maintain neural progenitors during Hensen's node progression. *Nat. Cell Biol.* **3**, 559-566.
Meinertzhagen, I. A. and Okamura, Y. (2001). The larval ascidian nervous system: the chordate brain from its small beginnings. *Trends Neurosci.* **24**, 401-410.
Meinertzhagen, I., Lemaire, P. and Okamura, Y. (2004). The neurobiology of the ascidian tadpole larva: recent developments in an ancient chordate. *Ann. Rev. Neurosci.* **27**, 453-485.
Miao, H., Wei, B. R., Peehl, D. M., Li, Q., Alexandrou, T., Schelling, J. R., Rhim, J. S., Sedor, J. R., Burnett, E. and Wang, B. (2001). Activation of EphA receptor tyrosine kinase inhibits the Ras/MAPK pathway. *Nat. Cell Biol.* **3**, 527-530.
Miller, A. C., Lyons, E. L. and Herman, T. G. (2009). cis-Inhibition of Notch by endogenous Delta biases the outcome of lateral inhibition. *Curr. Biol.* **19**, 1378-1383.
Nagatomo, K. and Fujiwara, S. (2003). Expression of Raldh2, Cyp26 and Hox-1 in normal and retinoic acid-treated Ciona intestinalis embryos. *Gene Expr. Patt.* **3**, 273-277.
Nicol, D. and Meinertzhagen, I. A. (1991). Cell counts and maps in the larval central nervous system of the ascidian Ciona intestinalis (L.). *J. Comp. Neurol.* **309**, 415-429.
Nishino, A., Okamura, Y., Piscopo, S. and Brown, E. R. (2010). A glycine receptor is involved in the organization of swimming movements in an invertebrate chordate. *BMC Neurosci.* **11**, 6.
Ohtoshi, A. and Behringer, R. (2004). Neonatal lethality, dwarfism, and abnormal brain development in Dmbx1 mutant mice. *Mol. Cell. Biol.* **24**, 7548-7558.
Pasini, A., Amiel, A., Rothbächer, U., Roure, A., Lemaire, P. and Darras, S. (2006). Formation of the ascidian epidermal sensory neurons: insights into the origin of the chordate peripheral nervous system. *PLoS Biol.* **4**, e225.
Peng, C. Y., Yajima, H., Burns, C. E., Zon, L. I., Sisodia, S. S., Pfaff, S. L. and Sharma, K. (2007). Notch and MAML signaling drives Scl-dependent interneuron diversity in the spinal cord. *Neuron* **53**, 813-827.
Picco, V., Hudson, C. and Yasuo, H. (2007). Ephrin-Eph signalling drives the asymmetric division of notochord/neural precursors in Ciona embryos. *Development* **134**, 1491-1497.
Pierfelice, T., Alberi, L. and Gaiano, N. (2011). Notch in the vertebrate nervous system: an old dog with new tricks. *Neuron* **69**, 840-855.
Reeber, S. L., Sakai, N., Nakada, Y., Dumas, J., Dobrenis, K., Johnson, J. E. and Kaprielian, Z. (2008). Manipulating Robo expression in vivo perturbs commissural axon pathfinding in the chick spinal cord. *J. Neurosci.* **28**, 8698-8708.
Rusch, J. and Levine, M. (1997). Regulation of a dpp target gene in the Drosophila embryo. *Development* **124**, 303-311.
Russo, M. T., Donizetti, A., Locascio, A., D'Aniello, S., Amoroso, A., Aniello, F., Fucci, L. and Branno, M. (2004). Regulatory elements controlling Ci-msxb tissue-specific expression during Ciona intestinalis embryonic development. *Dev. Biol.* **267**, 517-528.
Satoh, N. (2003). Ciona intestinalis: an emerging model for whole-genome analyses. *Trends Genet.* **19**, 376-381.
Satou, Y., Yamada, L., Mochizuki, Y., Takatori, N., Kawashima, T., Sasaki, A., Hamaguchi, M., Awazu, S., Yagi, K. and Sasakura, Y. (2002). A cDNA resource from the basal chordate Ciona intestinalis. *Genesis* **33**, 153-154.
Satou, Y., Kawashima, T., Shoguchi, E., Nakayama, A. and Satoh, N. (2005). An integrated database of the ascidian, Ciona intestinalis: towards functional genomics. *Zool. Sci.* **22**, 837-843.
Shi, W. and Levine, M. (2008). Ephrin signaling establishes asymmetric cell fates in an endomesoderm lineage of the Ciona embryo. *Development* **135**, 931-940.
Sprenger, F. and Nusslein-Volhard, C. (1992). Torso receptor activity is regulated by a diffusible ligand produced at the extracellular terminal regions of the Drosophila egg. *Cell* **71**, 987-1001.
Stolfi, A. and Levine, M. (2011). Neuronal subtype specification in the spinal cord of a protovertebrate. *Development* **138**, 995-1004.
Takahashi, T. and Holland, P. (2004). Amphioxus and ascidian Dmbx homeobox genes give clues to the vertebrate origins of midbrain development. *Development* **131**, 3285-3294.
Takamura, K., Egawa, T., Ohnishi, S., Okada, T. and Fukuoka, T. (2002). Developmental expression of ascidian neurotransmitter synthesis genes. *Dev. Genes Evol.* **212**, 50-53.
Takamura, K., Minamida, N. and Okabe, S. (2010). Neural map of the larval central nervous system in the Ascidian Ciona intestinalis. *Zool. Sci.* **27**, 191-203.
Tassy, O., Dauga, D., Daian, F., Sobral, D., Robin, F., Khoueiry, P., Salgado, D., Fox, V., Caillol, D. and Schiappa, R. (2010). The ANISEED database: Digital representation, formalization, and elucidation of a chordate developmental program. *Genome Res.* **20**, 1459-1468.
Thaler, J., Lee, S., Jurata, L., Gill, G. and Pfaff, S. (2002). LIM factor Lhx3 contributes to the specification of motor neuron and interneuron identity through cell-type-specific protein-protein interactions. *Cell* **110**, 237-249.
Thor, S., Andersson, S., Tomlinson, A. and Thomas, J. (1999). A LIM-homeodomain combinatorial code for motor-neuron pathway selection. *Nature* **397**, 76-80.
Wainwright, S. M. and Ish-Horowicz, D. (1992). Point mutations in the Drosophila hairy gene demonstrate in vivo requirements for basic, helix-loop-helix, and WRPW domains. *Mol. Cell. Biol.* **12**, 2475-2483.
Wilson, L. and Maden, M. (2005). The mechanisms of dorsoventral patterning in the vertebrate neural tube. *Dev. Biol.* **282**, 1-13.
Wong, L., Weadick, C., Kuo, C., Chang, B. and Tropepe, V. (2010). Duplicate *dmbx1* genes regulate progenitor cell cycle and differentiation during zebrafish midbrain and retinal development. *BMC Dev. Biol.* **10**, 100.
Zagoraiou, L., Akay, T., Martin, J. F., Brownstone, R. M., Jessell, T. M. and Miles, G. B. (2009). A cluster of cholinergic premotor interneurons modulates mouse locomotor activity. *Neuron* **64**, 645-662.